A STUDY ON TYPHOONS INDUCED NEARSHORE HYDRODYNAMICS ALONG KINMEN COAST

Wen-Son Chiang [1] Wei-Shiun Lu [2] Gia-Yun Chen [3] and Jin-Li Yu [1]

Coastal erosion along Liaolo Bay which is a semi-circular beach and locates at the south coast of Kinmen Island was observed during past years. Field and numerical experiments were conducted to discuss the hydrodynamics inside the bay. CMS-WAVE and CMS-FLOW models were setup and validated according to the collected field data. Then, the models were applied to simulate the hydrodynamics inside the study site during typhoon events. Longshore current pattern along the semi-cicular beach is sensitive to the incident wave. For wave approaching from east direction, the most affected region inside the bay by the wave locates on the west of the beach. However, widespread impact on the whole beach was found when the wave incident from south direction. Wave (1~2 m) travels from E~ESE direction at the bay mouth usually occurs in winter and induces to consistently westward lognshore current along the beach with speed 0.2~0.4 m/s. High wave approached from SE~S direction during the studied typhoon events which induced to strong transiently and complex current patterns inside the bay beach with maximum speed up to more than 1.0 m/s. A rip circulation cell constantly found near the outcrop, which enhanced the strength of the rip circulation. Besides, rip circulation cells occasionally found at some spots along the beach respectively which depends on the incident wave energy and direction.

Keywords: longshore current; typhoon; coastal erosion

Introduction

Kinmen County is located on the southeast coast of mainland China. It is a small archipelago of several islands and comprises two large islands, Kinmen and Lieyu. It is geographically very near Xiamen, no more than 2 km (Fig. 1). Quemoy is the name for the island in English and in many European languages. A martial law was imposed on the island before 1992. Because of its military consideration, development on the island was extremely limited. In 1992, the martial law was abolished and the economy transitioning from military rule to tourism. As a result, it is now a popular weekend tourist destination for Taiwanese and is known for its quiet villages, old-style architecture, and beaches. Accompany with the fast development of tourism, a large demand of flight transportation need to be satisfied. So, the Kinmen Airport underwent two extensions during past 10 years and the runway extension is now under consideration. However, the original constructed runway located several hundred meters away from a bay beach. Nowadays, the distance between eastern part of its runway and the beach is only one to two hundred meters due to beach erosion during past several decades (Fig. 2). Over the past few years, beach erosion off the runway which locates at the southeast coast of Kinmen Island became more serious than ever. In general, beach erosion is related to nearshore hydrodynamics, bathymetry, coastal structures and sand resources availability. In order to protect the coast from further erosion, varied coastal structures were constructed during past few years. However, part of the coastal protection structures were collapsed gradually or accidently due to the hydrodynamic forces driven by typhoon events occurred during past years. Especially in 2010, two typhoon events, namely Fanabi and Magi, affected the coastal area of Kinmen Islandand induced to large scale coastal protection structures failure. A further coastal protection project is urgent for the coast.

Study site

LiaoLo Bay is a south-facing semi-circular beach on the Kinmen Island. The 8 kms of sandy beaches extend from southwestern end to the northeastern end of the island. The sandy beach evolves naturally and eroded constantly in past. To clarify the potential factors related to the coastal erosion, field investigations were conducted along the southern coast of Kinmen Island to collect the nearshore hydrodynamic and the sediment parameters.

The slope of seabed profile is roughly 1:40 in shallow water and it approaches 1:700 for far offshore. Surface sediment samples distributed along the coast and offshore were analyzed and the median grain size (D_{50}) of the sediments decreases with depth increasing (figure 3). In the surf zone, the main constituent of the sediment is sand and D_{50} ranges between 0.178 mm and 0.257 mm. For deeper area, the marine sediment is basically distributed silt although some mixtures of sand and silt found at few specific locations. Mean tidal range is 4.5 m near the study site.

For current velocity and wave climate measurements, acoustic Doppler current profile was deployed at 8 m depth during May and July, 2013. The main current direction was NE for ebb flow and

[1] Researcher, Tainan Hydraulics Laboratory, National Cheng Kung University, Taiwan
[2] Research Assistant, Tainan Hydraulics Laboratory, National Cheng Kung University, Taiwan
[3] Assistant Researcher, Tainan Hydraulics Laboratory, National Cheng Kung University, Taiwan

SW for flood flow and was dominant by astronomical tides. As to the magnitude of the current, about 50% of the collected data were less than 12.5 cm/s.

Summer wave conditions tend to be calm, dominated by southwest wind that generates wave height less than 1m. Winter conditions are dominated by northeast wind (high pressure systems originated from Siberia) generating wind waves 1.5 m in average and last for several months. The largest wave heights up to 9m, are produced during the storm events, originating from the low pressure systems near the southwest Pacific Ocean. Although the Liaolo Bay is a semi-enclosed bay, storms propagating from southern Taiwan Strait can generate powerful wind swells, as shown in figure 4, the time series of in-situ wave data recorded in year 2010 off the bay mouth.

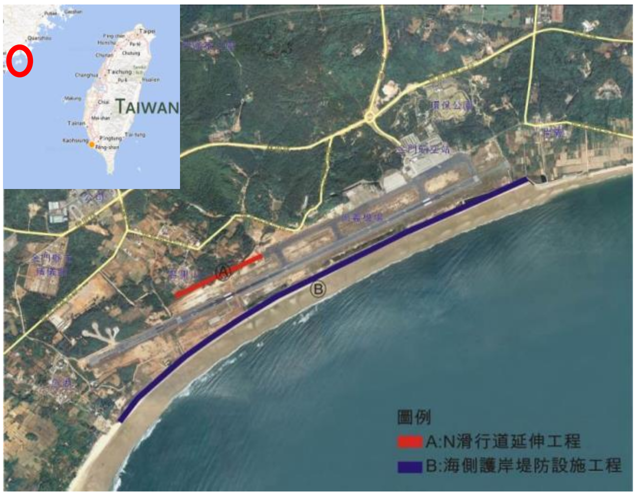

Fig. 1 location of the Kinmen Island and Liaolo Bay at the south coast of the island.

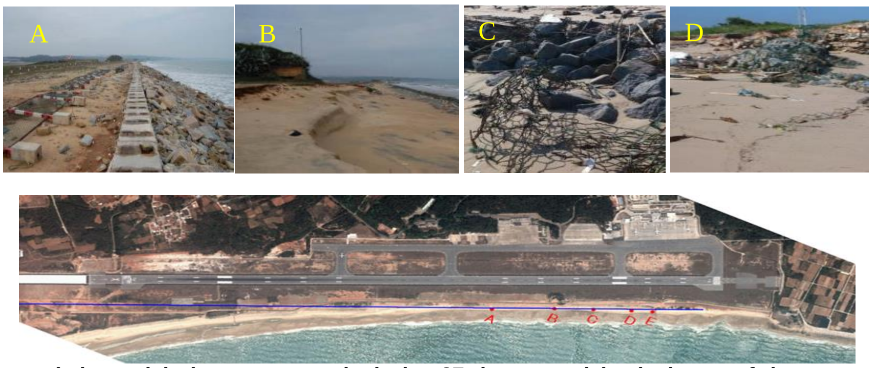

Figure 2 (bottom) the aerial photo, rotates clockwise 27 degree and (top) photos of the coastal protection structures along the study site

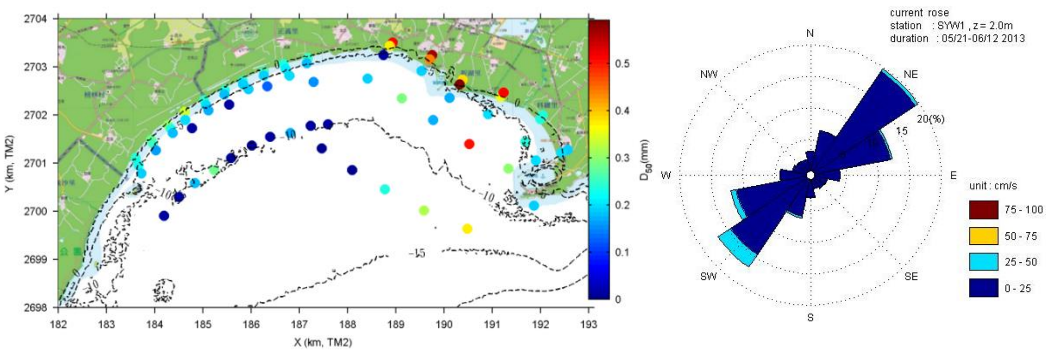

Figure 3 (a) spatial distribution of seabed sediments, D_{50} inside the Liaolo Bay (b) current rose recorded at wave buoy 46787A

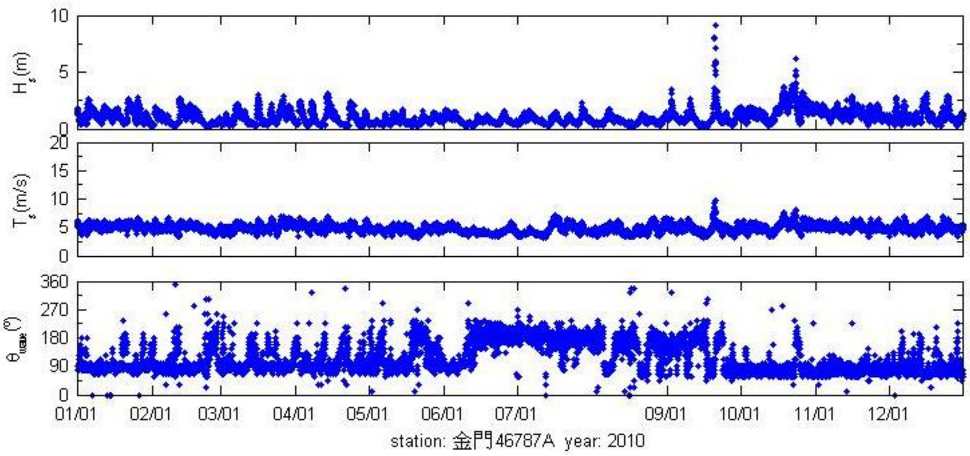

Figure 4 time series of wave data recorded by wave buoy 46787A at the Liaolo bay mouth

Model setup and calibration

Because of the dynamic variations of the strong winds and waves, it is usually difficult to investigate the mechanics of typhoon impacts on coastal area by limited field observations. Numerical modeling, after validated, provides a viable approach to investigate the forcing and induced transport process during typhoon events. By using the collected field data, the numerical models were setup, verified and then applied to the coastal area of Liaolo Bay in order to reproduce the nearshore hydrodynamics during typhoon events occurred in year 2010. Model predictions of wave and current fields at different time instants during the typhoon events were used to analyze the temporal and spatial variations of flow circulation inside the bay. The numerical models, CMS-FLOW and CMS-WAVE, which developed by the U.S. Army Corps of Engineers were used to simulate the current and wave motion. The CMS-FLOW model is a time dependent, 2-D finite volume model that calculates water surface elevation, two-components of the current. The CMS-WAVE is a nearshore spectral wave transformation model (Sanchez et al., 2012).

The model domain extended approximately 12 km alongshore and 11.6 km offshore to a depth of 30 m (see figure 5). The bottom topography dataset consisted of high resolution nearshore survey data collected in 2013 by Tainan Hydraulics Laboratory. Coordinates were set to TM2 (horizontal) and TWD97 (vertical) in meters. Grid cell size was uniform, 40 m. The wave model was coupled to the circulation model at 1 hour interval.

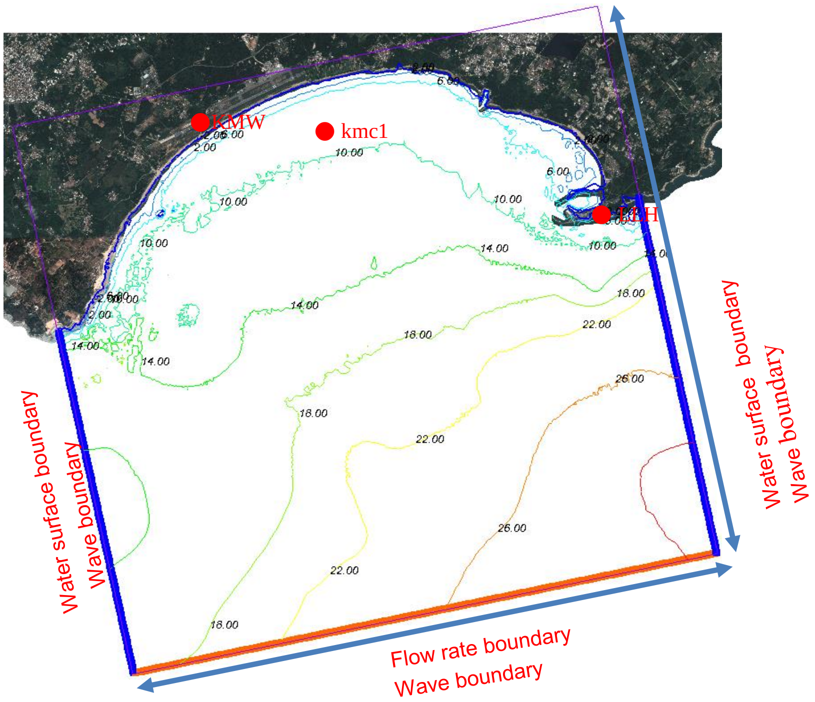

Figure 5 hydrodynamics model domain

The circulation model was forced by in-situ water level data obtained from Central Weather Bauru, Taiwan. The wave model simulations were driven by in-situ wave data recorded near the bay mouth by Water Resource Agency, Taiwan. The model results were verified by comparison with the field data collected during May and June, 2013. As shown in figure 6, model predictions of water levels and current velocities match well with the observation at shallow water, kmc1 station near the center of the bay beach. The satisfactory reproduction of the water level and current driven by wind, wave and tide indicates that the coupled model is capable of predicting reasonably the coastal circulation inside the bay. Model predictions of wave height and direction at kmc1 station are presented in figure 7. In general, model simulation of wave height is in good agreement with observations. Simulated wave direction matches well with the general trend of the observed data in spite of some minor difference found at some specific time. To verify the difference between the measured and simulated time series, indices for agreement (*D*) and the average deviation (*P*) were applied according to the method of Willmott(1981), in which *D* and *P* indices are defined as follows. A summary of statistics for model validation for wave and current simulation is given in table 1.

$$D = 1 - \frac{\sum_{n=1}^{N}(P_n - O_n)^2}{\sum_{n=1}^{N}(|P_n - O| + |O_n - O|)^2} \tag{1}$$

P_n is the predicted value, and O_n and O are the measurements and measurement averages, respectively. The average deviation *P* is defined as follows.

$$bias(P) = \frac{\sum_{n=1}^{N}(P_n - O_n)}{\sum_{n=1}^{N} O_n} \tag{2}$$

Table 1 A summary of statistics for model validation for wave and current simulation

item	*D*	bias(*P*), %
surface elevation	0.998	0.256
velocity-E	0.962	-5.926
velocity-N	0.908	-1.740
Wave height	0.913	0.043

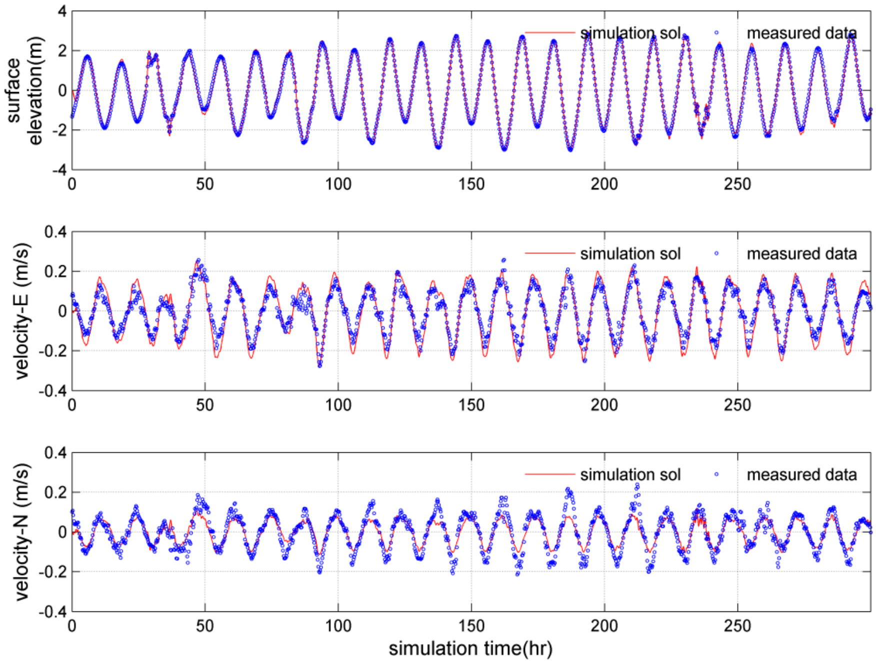

Figure 6 comparisons of the water level and current velocity at the site kmc1 between the measured and simulated results.

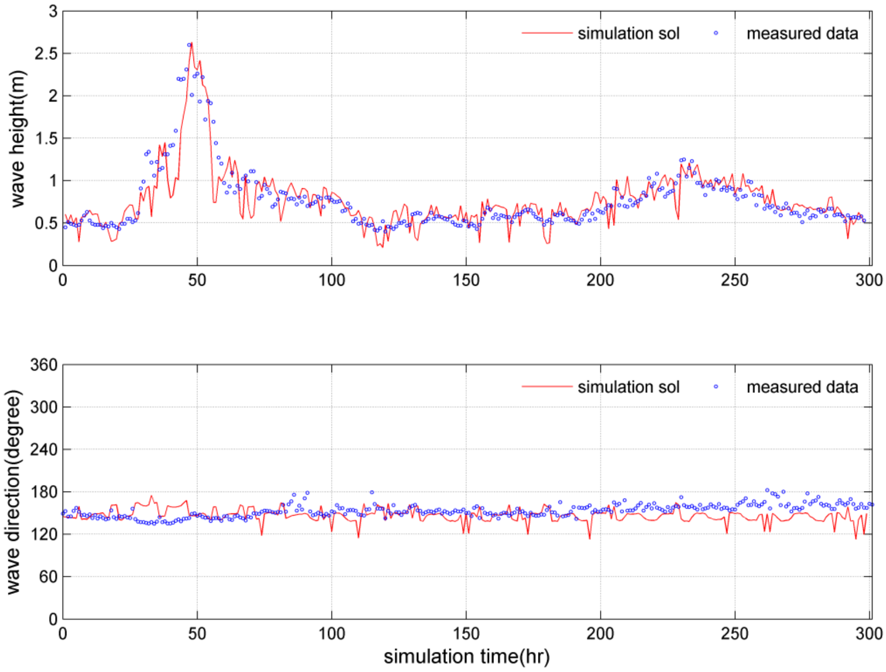

Figure 7 comparisons of the wave height and direction at the site kmc1 between the measured and simulated results.

Typhoon events

To understand the hydrodynamics inside the Liaolo Bay during typhoon impact period, the verified numerical models were applied to the study site. The measured wave and tidal data during Typhoon Fanabi and Magi in 2010 were used to force the CMS-WAVE and CMS-FLOW models, respectively. Figure 8 indicates the weather and coastal water conditions during the typhoon events recorded at statinos LLH and KMW (shown in figure 5). Typhoon Fanabi occurred in late Sep., 2010. A typical summer weather condition, low wave and light wind, previaled the pre-typhoon time period. At most extreme condition induced by the typhoon, wave height approached to 9.12 m from southeast at the bay mouth.

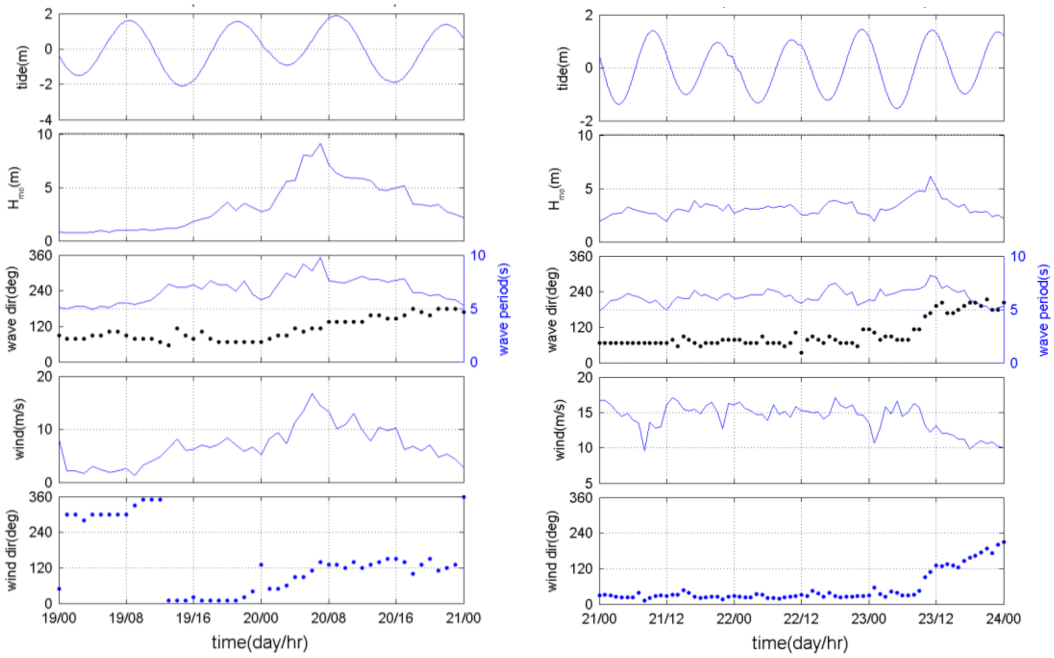

Figure 8 measured coastal wave(buoy 47687A), tide(LLH) and wind(KMW) conditions during typhoons (left) Fanabi and (right) Magi.

Typhoon Magi occurred in late October, 2010. Before the typhoon affecting the study site, Waves driven by winter monsoon dominated and propagated from northeast at offshore. Waves with height 2~3 m and direction ~90^o were recorded at depth 25 m near the bay mouth. When Typhoon Magi moved close to the study site, the recorded wave height increased gradually until a maximum roughly 6 m from south and wind direction shifted from northeast to southeast.

Results and discussions

The Liaolo Bay is a south-facing bay locates at the south boundary of Kinmen Island, most of the wave approaching from northeast was block and therefore much smaller wave was found inside the bay in strong winter monsoon season. The most widespread wave impact was simulated for waves approaching from the south. The incident high wave approached nearshore without damping because the local geomorphology exhibited a very mild slope for deep water (> 8 m) and a steeper slope for shallow water. The following analysis discusses model results of the simulation of typhoon events, Fanabi and Magi.

In figure 9 ~ 12, snapshots of spatial wave heights and currents at different time instants during Typhoon Fanabi, along with wind and tide focing, are investigated to show the impacts on the coastal area.

Figure 9 shows wave height and current at flooding tide with light wind (2 m/s) before the arrival of the typhoon. It is a typical condition in summer. The wave height was low, less than 1 m and current directed to southwestward along the beach with magnitude smaller than 0.2m/s during flooding tide except near the headlands where stronger current found.

Figure 10 exhibits the results at the beginning of the rising limb of the wave height during ebb tide with wind speed of 8.3 m/s from 50^o. Ebb tide pushed the northeastward movement of the bay water. Meanwhile, wave originated from northeast with magnitude 3 m due to wind forcing and propagates into the shallower bay from east through deflection and diffraction due to bathymetry effect. Focusing of wave energy were found at some portions of the bay which enhanced the longshore current after wave breaking. However, the wave induced current was balanced off by the tidal and wind driven current. So, almost calm flow was found near the coast, especially east portion of the beach.

At the maximum wave height, 9.12 m from 112^o, during Typhoon Fanabi (Fig. 11), wind speed was 14 m/s from 140^o during flooding tide. For the east of the outcrop near Houhu combination of the hydrodynamic forcing due to breaking wave and flooding tide pushed the costal water southwestward with magnitude up to 0.6 m/s. However, the longshore current, mainly driven by wave breaking, along the west beach of the outcrop showed a predominance of northeast. Thus, a rip current system occurred near the outcrop which could lead to an offshore sediment transport.

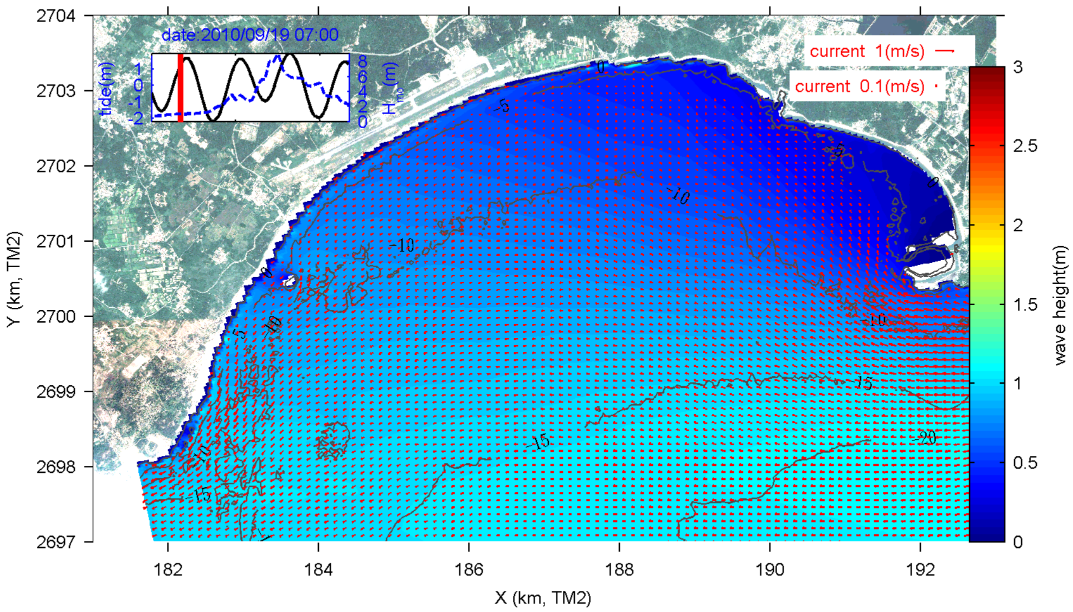

Figure 9 snapshot of spatial wave heights and currents at a time (7:00 Sep., 19, 2010) during Typhoon Fanabi (wind speed and direction: 2m/s, 300^o, wave height and direction: <1.0m, 95^o)

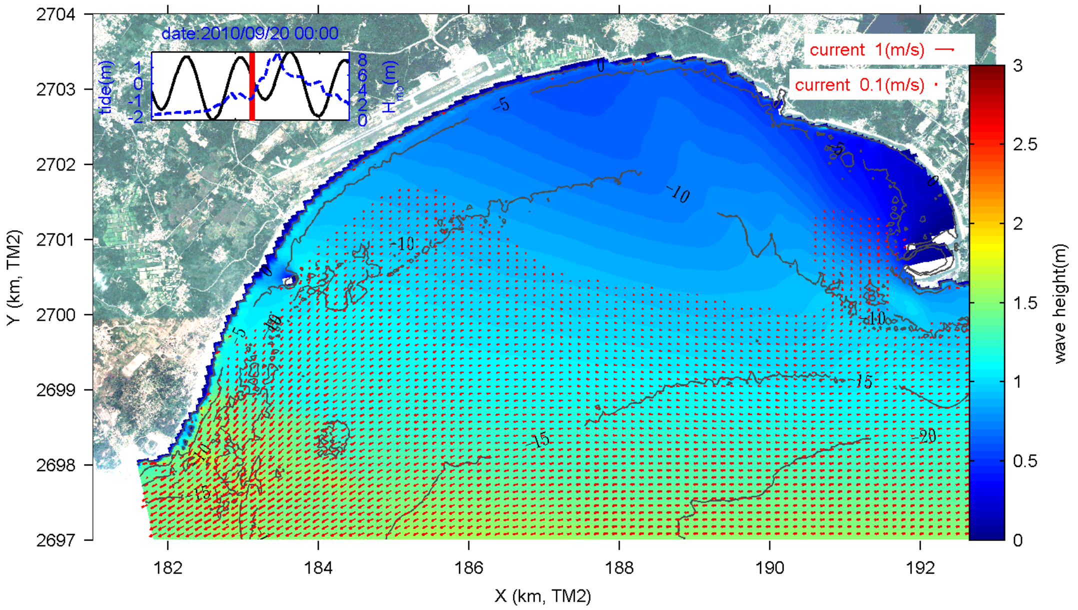

Figure 10 snapshot of spatial wave heights and currents at a time (0:00 Sep., 20, 2010) during Typhoon Fanabi (wind speed and direction: 6m/s, 60°, wave height and direction: 3m, 45°)

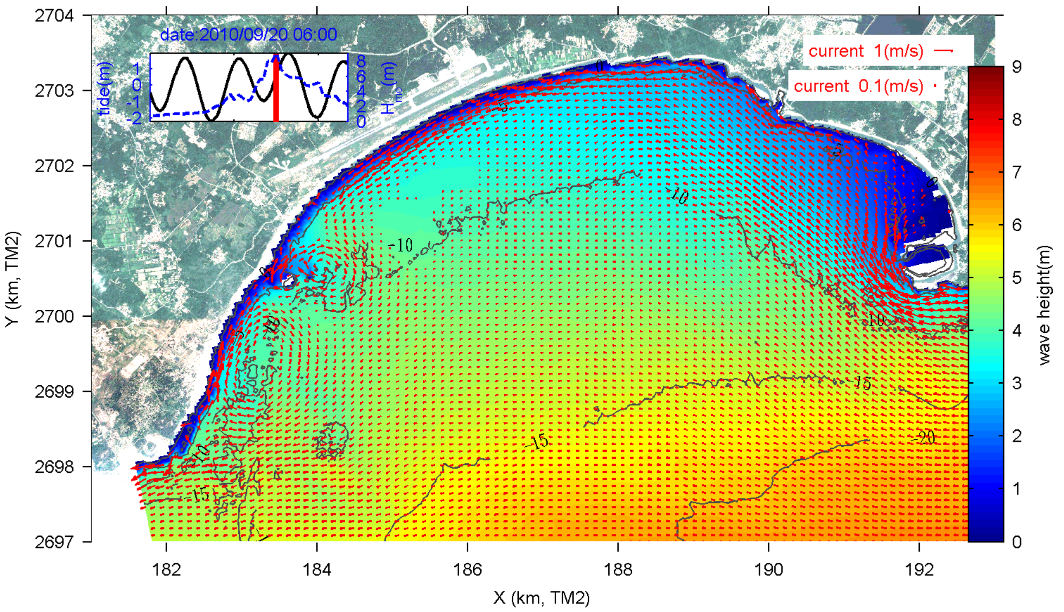

Figure 11 snapshot of spatial wave heights and currents at a time (6:00 Sep., 20, 2010) during Typhoon Fanabi (wind speed and direction: 14m/s, 140°, wave height and direction: 9.12m, 112°).

Figure 12 shows a snapshot at the lower end of the falling limb with wind speed 5 m/s and wave height 3.3 m from 180° during Typhoon Fanabi. Currents off the coast dominated by flooding tide and went to southwest. Wave impacted on east of the bay beach from southeast/south due to topography effect. But the wave direction shifted to south/southwest on west of the beach. The change in incident wave direction induced to the reversal longshore current. Two rip current cells were found at the west and east part of the bay beach, respectively.

The following analysis show snapshots of wave height and current at some time instant during Typhoon Magi. Figure 13 shows a typical wave pattern inside the bay in winter. Wave generated by NE monsoon with speed 15 m/s, which propagated from offshore with magnitude 3 m and was block by the headland located east of the study beach. In general, wave height was less than 1 m inside the bay except the western side of the bay beach where widepread impact from diffracted wave was found. The longshore current with magnitude 0.2~0.4 m/s basically directed to southwest along the beach. At the maximum wave height, 6.12 m, and direction 168° during Typhoon Magi (figure 14), wind speed was 13 m/s from 120^o during flooding tide. In general, the current pattern and also weather and sea conditions were similar to those in figure 12, although, the wind was stronger and wave was higher. It demonstrates that south incident wave tends to induced to two rip circulation cells near Hohu and Chengkung, locates at the west and east part of the bay respectively.

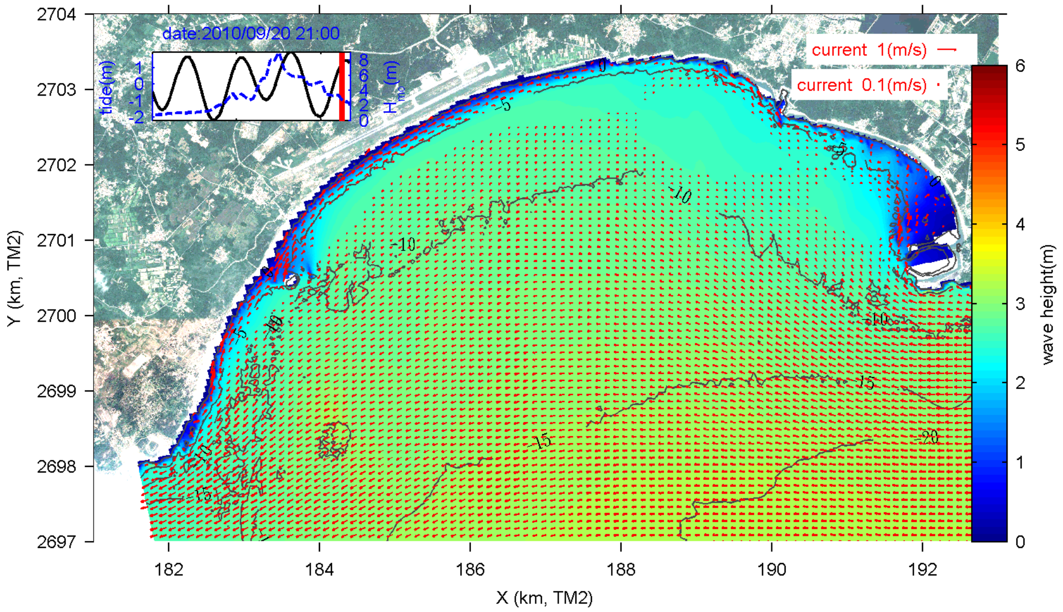

Figure 12 snapshot of spatial wave heights and currents at a time (21:00 Sep., 20, 2010) during Typhoon Fanabi (wind speed and direction: 5m/s, 115^o, wave height and direction: 3m, 180^o)

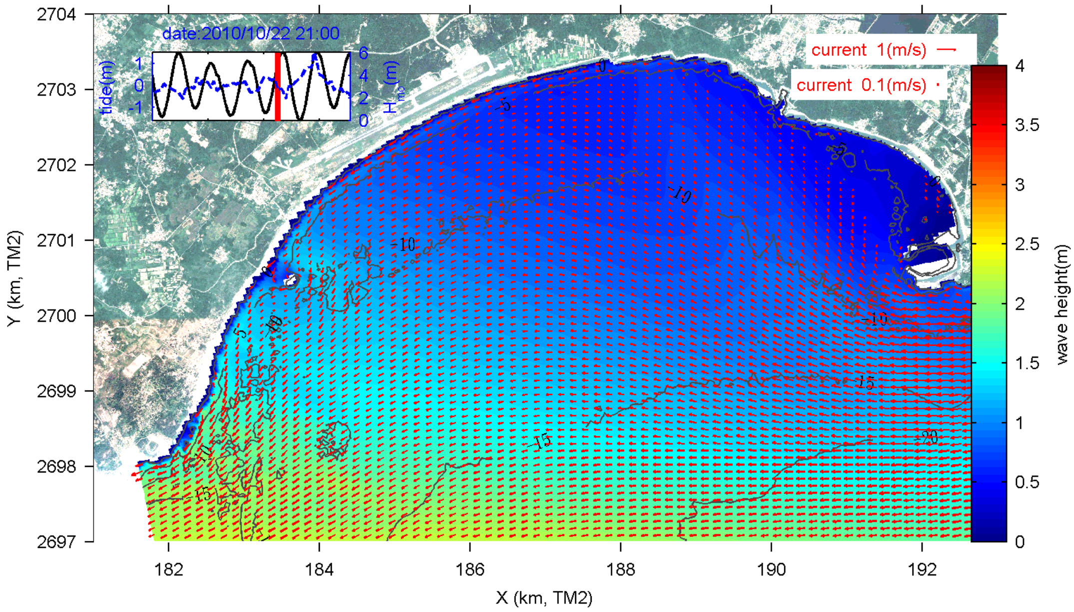

Figure 13 snapshot of spatial wave heights and currents at a time (21:00 Oct., 22, 2010) during Typhoon Magi (wind speed and direction: 15m/s, 45^o, wave height and direction: 3m, 95^o)

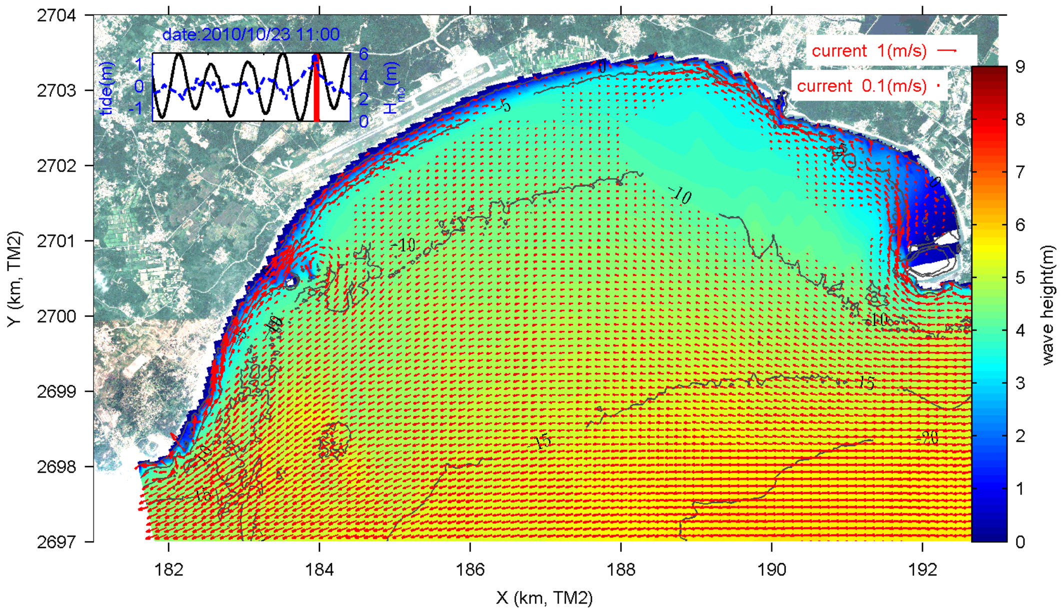

Figure 14 snapshot of spatial wave heights and currents at 11:00 Oct. 23, 2010 during Typhoon Magi (wind speed and direction: 13m/s, 120^o, wave height and direction: 6.12m, 128^o)

Comparisons of wave roses at varied location along the beach

Wave roses at ten stations along the beach based on simulated results during the typhoon events were extracted and shows in figure 15. The figure shows evidently different wave distribution for varied site locates east vs. west of the bay beach, which is of great interest because a change in wave direction can lead to a reversal in the direction of induced longshore current. The wave height distribution on the east of the beach showed a predominance of wave approaching from S and shifted gradually to the ESE on the west of the beach.

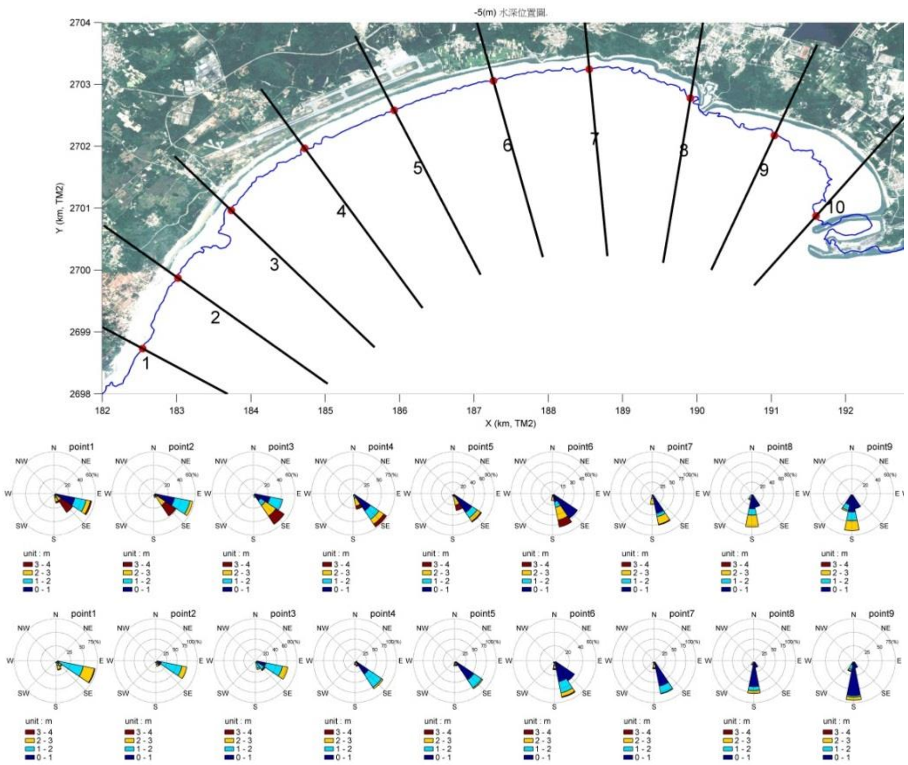

Figure 15 Comparisons of wave roses at varied location along the beach during Typhoon events (upper: Fanabi, lower: Magi).

Comparisons of current roses at varied location along the beach

The spatial distribution of simulated current field at varied loactions along the beach duing Typhoon Fanabi and Magi are compared in figure 16. In general, the results demonstrate that the longshore currents on the west of the beach were sensetive to the approaching wave direction. Incident wave from E~ESE induced the longshore current directed to NE. However, wave approached from SE~S, the southwestward longshore currents were found. For the central part of the beach, longshore current was almost consistent and dominated by the W~SW direction. Complicated variation of longshore current on the east was found due to some harbour seawalls were constructed along the beach.

The typhoon events induced wave heights and current speeds extracted along a transect running from southwest to northeast of Liaolo Bay are compared in figure 17 and 18. Figure 17 shows comparison of simulated wave statistics at varied locations along the beach during typhoon events, Fanabi and Magi. Generally, widespread impact wave was found on the west of the beach. However, the occurrence probability distribution of modelled wave height was different between these two events, which were related to the pre-storm weather conditions, especially wind condition. In winter, the wind is relatively stable and constantly from NE direction. However, wind is weak and direction is transient in summer. So, peak of the probability distribution function of wave height was much higher in winter than that in summer. Longshore current speed distribution along the coast during the typhoon events is shown in figure 18. Corresponded to the impact wave height, the longshore current was stronger on the west of the beach. Some local variations of current speeds exhibited close to the coastal structures, for example the outcrop at 183.5 km and the harbor seawalls at 190 km. At the central part of the bay beach, off the airport runway, the current speed was smoothly distributed.

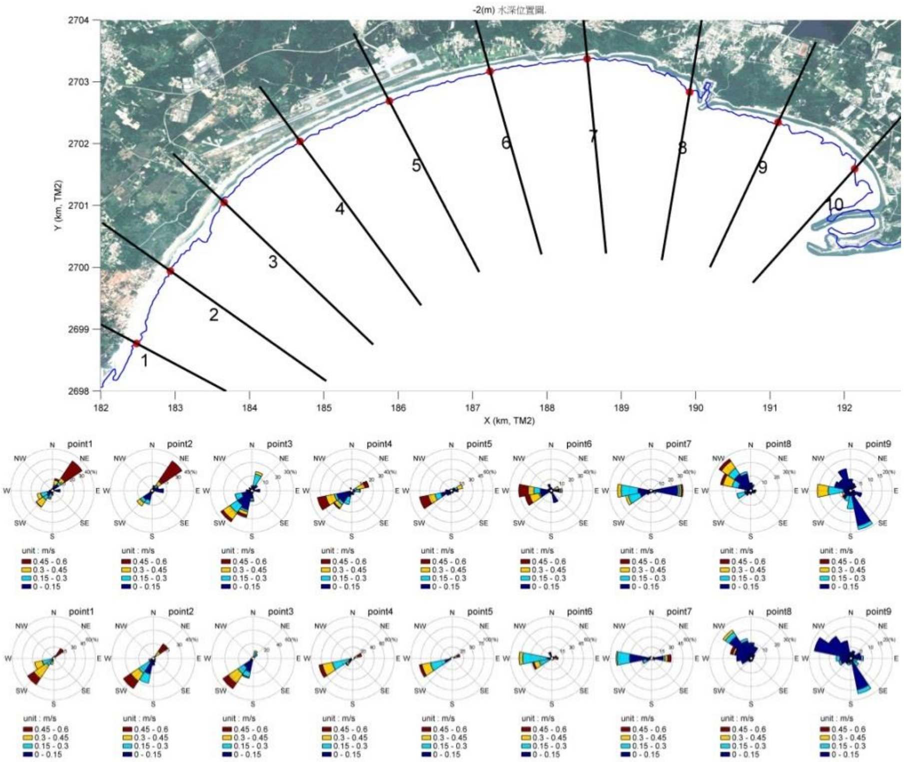

Figure 16 Comparisons of current roses at varied location along the beach during Typhoon events (upper: Fanabi,;lower: Magi).

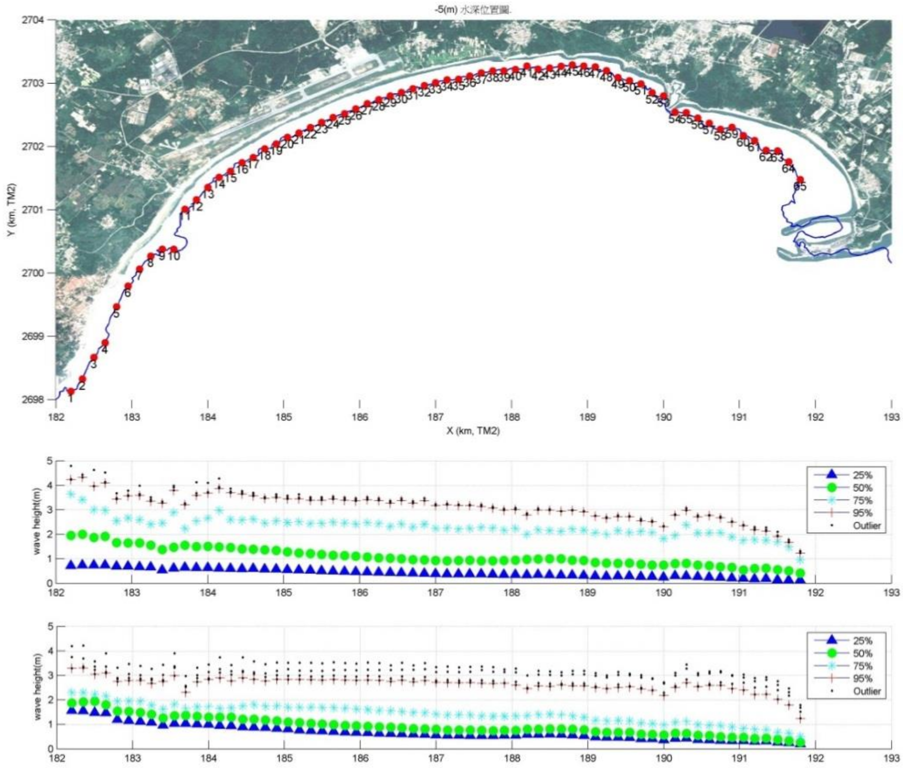

X(km, TM2)

Figure 17 wave heights extracted along a transect running from southwest to northeast of Liaolo Bay (upper: Fanabi, lower: Magi). Different symbol represents the wave height corresponded to xx% of accumulative probability

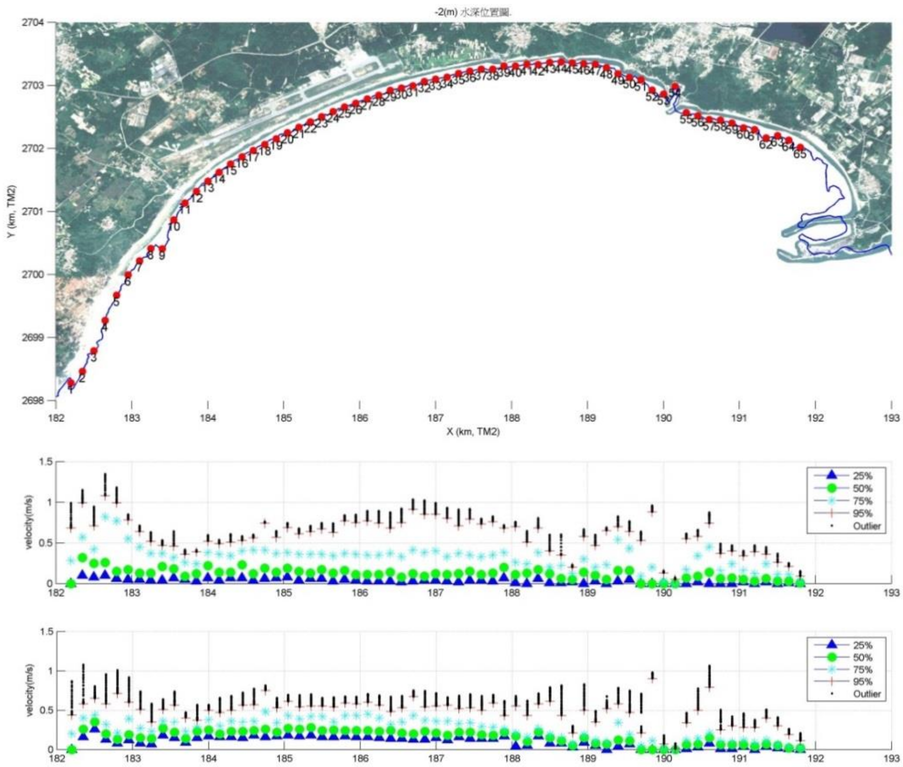

X(km, TM2)

Figure 18 current speeds extracted along a transect running from southwest to northeast of Liaolo Bay (upper: Fanabi, ;lower: Magi). Different symbol represents the wave height corresponded to xx% of accumulative probability

Conclusions

Longshore current pattern along the semi-cicular beach, Liaolo Bay, was sensitive to the incident wave based on the numerical study results. For wave approaching from east direction, the most affected region inside the bay by the wave locates on the west of the beach. However, widespread impact on the whole beach was found due to the wave incident from south direction. Wave (1 ~ 2 m) travels from E ~ ESE direction at the bay mouth usually occurs in winter and induces to consistently westward lognshore current along the beach with speed 0.2 ~ 0.4 m/s. High wave up to more than 6 m approaches from SE ~ S direction occassionally occurred during typhoon events. Therefore induced to strong transiently and complex longshore current pattern inside the bay beach with maximum speed up to more than 1.0 m/s. A rip circulation cell constantly found near the outcrop, which enhanced the strength of the rip circulation. Besides, rip circulation cells occasionally found at some spots along the beach respectively which depends on the incident wave energy and direction.

REFERENCES

Sanchez, A., Lin, L., Demirbilek Z., Beck, T., Brown, M., Li, H., Rosati, J., Wu, W. and Reed, C., 2012, Coastal modeling system draft user manual., Coastal Hydraulics Laboratory, U.S. Army Engineer Research and Development Center.

Brehin, F., Zarillo, G., Flanary C., Jerry, N, Gouaud, F., Charriere A., 2013, Hydrodynamics and morphological modeling of La Napoule Bay, France., *Proceeding of 7th Coastal Dynamics Conference*, pp. 203-212.

Willmott, C.J., 1981. On the validation of models, *Physical Oceanography*, Vol. 2(2), pp. 184-194